International Journal of Mechanical, Industrial and Aerospace Sciences
ISSN: 2517-9950
Vol:10, No:1, 2016

# Super-ellipsoidal Potential Function for Autonomous Collision Avoidance of a Teleoperated UAV

Mohammed Qasim, Kyoung-Dae Kim

*Abstract*—In this paper, we present the design of the super-ellipsoidal potential function (SEPF), that can be used for autonomous collision avoidance of an unmanned aerial vehicle (UAV) in a 3-dimensional space. In the design of SEPF, we have the full control over the shape and size of the potential function. In particular, we can adjust the length, width, height, and the amount of flattening at the tips of the potential function so that the collision avoidance motion vector generated from the potential function can be adjusted accordingly. Based on the idea of the SEPF, we also propose an approach for the local autonomy of a UAV for its collision avoidance when the UAV is teleoperated by a human operator. In our proposed approach, a teleoperated UAV can not only avoid collision autonomously with other surrounding objects but also track the operator's control input as closely as possible. As a result, an operator can always be in control of the UAV for his/her high-level guidance and navigation task without worrying too much about the UAVs collision avoidance while it is being teleoperated. The effectiveness of the proposed approach is demonstrated through a human-in-the-loop simulation of quadrotor UAV teleoperation using virtual robot experimentation platform (v-rep) and Matlab programs.

*Keywords*—Artificial potential function, autonomy, collision avoidance, teleoperation, quadrotor, UAV.

## I. Introduction

IN the recent years, due to various advantages in terms of their size, cost, weight, and, more importantly, versatile mobility such as hovering, vertical take-off and landing (VTOL), omnidirectional agile movement, etc., quadrotors UAVs have gained a lot of attention from scientists and have been used successfully in many tasks such as search and rescue, remote sensing, mapping, exploration, surveillance and many other civil and military applications [1], [2], [3], [4]. However, nowadays robots autonomy is still restricted by the deficiency of a robust and reliable perception, and of a higher cognitive abilities that permits sophisticated decision making in real world environment [5]. Thus, human supervisory is required to perform high level decision making while the robots execute their local autonomy such as obstacle avoidance. In this context, [6], [7] represent an effective way to integrate robot local autonomy and human supervisory.

In teleoperation, the operator is physically separated from the robot. This leads to a difficult teleoperation process due to poor situation awareness [8]. One main way to transfer the information to the operator is through a camera mounted on the UAV. This visual information is often restricted due to limited camera resolution and field of view (FOV) [9]. In the case of quadrotor UAV, the teleopration is usually non-trival due to its inherent nonlinear underactuated dynamics, fast and agile omnidirectional mobility, etc. If a quadrotor UAV is not controlled carefully, it can easily collide with obstacles, especially in a cluttered indoor environment. And therefore it requires a high level of expertise as well as enough training to teleoperate a quadrotor UAV safely. This is our main motivation to develop an algorithm that assists the operator by making the robot avoid collision autonomously.

In our algorithm, operator commands that are only in the direction of obstacle are overridden and others that are in the obstacle free path are tracked. In this way, our algorithm ensures that: i) the UAV autonomously avoids obstacle in its path; ii) the UAV chooses the obstacle-free path if there is a control input in that path direction; and iii) the operator is always in control of the vehicle. Thus, our algorithm indeed enables easy and safe teleoperation.

The main contributions of this work are summarized as follows: First, we present a 3-dimensional potential function, which is called the *super-ellipsoidal potential function (SEPF)*, that generates motion vectors to avoid collisions. Second, we also present a simple yet very effective strategy that seamlessly incorporates motion commands from both the operator and potential functions for collision avoidance. Third, the proposed algorithm is implemented in a human-in-the-loop simulation environment using virtual robot experimentation platform (v-rep) and Matlab programs and its effectiveness is validated through simulations. Several different cases were implemented in an indoor environment where an operator attempts to collide a UAV with walls. Simulation results demonstrate that the UAV autonomously avoids the collision and followed the obstacle free path.

The rest of this paper is organized as follows: Section II presents the related work. Section III introduces the SEPF. Section IV states autonomous collision avoidance under teleoperation. Section V shows simulation results, and finally, Section VI concludes this paper and states some future works.

## II. Related Work

Collision avoidance is one of the essential tasks for mobile robots. Therefore, collision avoidance has been widely studied in the literature. Potential function based methods [8], [10]-[12] are developed for collosion avoidance in a UAV teleoperation. In [13]-[17], teleoperation with force feedback as a cue for the operator to increase the situation

Mohammed Qasim is with the Department of Electrical and Computer Engineering, University of Denver, Denver, Co, 80210 USA (e-mail: Mohammed.Qasim@du.edu).

Kyoung-Dae Kim is with the faculty of Department of Electrical and Computer Engineering, University of Denver, Denver, Co, 80210 USA (e-mail: Kyoung-Dae.Kim@du.edu).

awareness has been studied and applied to mobile robots to navigate in a cluttered environment. Potential function for collosion avoidance in a group of UAVs has been studied and implemented in [18]-[20]. Several research on the area of the assisted teleoperation by means of collision avoidance for UAVs has been conducted in recent years. The haptic device is used in [21] which provides a force feedback that can be interpreted by the operators as an impedance to their control input if the collision will occur in the near future. This assists the oprators to avoid collision. The amount of feedback force is proportional to the time to impact, which is the robot's current velocity divided by the relative distance to the nearest obstacle. The method of [22] uses a similar way to the method used in [21] by calculating the time to collision (TTC), which is similar to the time to impact. The difference is that the SLAM is used to map the environment and calculate the relative distance to the obstacle. TTC is classified into threat levels and the response, i.e., no action; slow; stop and evasive manoeuvre, is taken accordingly to override the operator control input and slow, stop, or move the robot oppositely to its current direction. The authors of [23] use a different approach from [21] and [22]; they take into account the actual dynamics, states, and the operator command input to estimate the future trajectory of the quadrotor UAV, and they use this trajectory to minimize the deviation from control input to automatically avoid collision with obstacles. However, the SLAM is required for this method to work. It can be seen that first two methods [21] and [22] do not take the robot dynamics into account and their algorithm overrides the operator command and stops the robot. In addition, method [22] is computationally expensive because it requires a SLAM to work. While method [23] performs automatic collision avoidance, it only works in a 2-dimensional space and is computationally expensive due to the SLAM process. In this paper, we address all the above problems. Our algorithm works in a 3-dimensional space, takes the vehicle's dynamics into account, does not require a SLAM, autonomously avoids obstacles, and ensures that the operator is in the control of the vehicle at all times.

## III. Super-Ellipsoidal Potential Function

A potential function is defined as a differential real valued function $P : \mathbb{R}^m \rightarrow \mathbb{R}$ and it was first introduced by Khatib [24], [25]. In robot motion planning literature, the gradient of a repulsive potential function typically represents a motion vector ($\mathbf{V}_{ca}$) that avoids collision with obstacles. In designing such a repulsive potential function, it must be ensured that a vehicle will not collide with other objects under any circumstances as well as avoids any undesirable motions. More specifically, when a vehicle is teleoperated, a vehicle should be stationary regardless of its relative distance to an obstacle when there is no motion command from an operator and also, more importantly, a vehicle should be able to stop before an obstacle no matter how fast it is approaching to the obstacle. In this section, we present the super-ellipsoidal potential function, SEPF, which provides enough flexibility in terms of designing the size and shape, and also addresses all of above mentioned issues.

### A. Design of The SEPF in a 2-Dimensional Space

We begin this section with the following assumptions:

1) The UAV is a rotary wing UAV type that can move in any direction in a 3-dimensional space.
2) The UAV is equipped with a sensor that can detect obstacles around the robot within a sphere of radius (Rs) as a point cloud.
3) The UAV has dynamics that are the same in every direction with a constant deceleration limit [8].

First, to include the vehicle dynamics in the design of a repulsive potential function, we take into account the minimum required distance ($d_{min}$), which is the distance for a vehicle to decrease its velocity to zero using the vehicle's maximum deceleration ($a_{max}$) allowed in the direction of motion, that is given by

$$d_{min} = \frac{\|\mathbf{v}\|^2}{2a_{max}} \tag{1}$$

where $\mathbf{v}$ is the current vehicle velocity. In addition, to remove the undesirable/unnecessary collision avoidance motion vectors due to surrounding obstacles: i) when there is a motion command input from an operator, we assign repulsive potential functions centered at the vehicle only in the direction of motion and an operator's motion command input; and ii) when there is no motion command input from an operator, we reduce the the length of the repulsive potential function and make it equal to its width as shown in Fig. 3.

As briefly mentioned above, we construct a repulsive potential function, called SEPF, using a pair of super-ellipses as shown in Fig. 1. One main advantage of using super-ellipse in the design of a potential function is that we can easily adjust the the length ($a$), width ($b$), and the amount of flattening ($n$) at the SEPF tips. As can be seen from Fig. 1, an SEPF is consisted of an inner and outer two halves of a super-ellipse centered at the center of the vehicle. The length ($a_{fo}$) of the outer half super-ellipse in the front direction of a vehicle is designed to be equal to the maximum distance sensor range when there is a motion command from an operator and to be equal to its width ($b_{fo}$) when there is no motion command from an operator. The width ($b_{fo}$) of the same front half

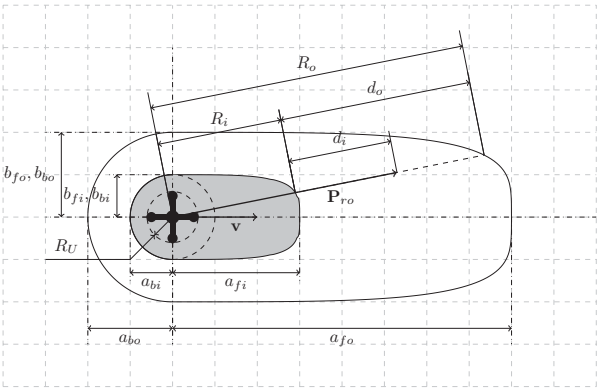


Fig. 1 Representation of a 2-dimensional SEPF, showing the control parameters and variables

super-ellipse is chosen to be, at least, two times greater than the radius ($R_U$) of the smallest circle that encircles the UAV (See Fig. 1). Another outer half super-ellipse facing toward the back of a vehicle has length ($a_{bo}$) that is equal to its width ($b_{bo}$) to form a half circle behind the vehicle. To ensure the continuity between the two outer half super-ellipses, the width of the backward facing super-ellipse ($b_{bo}$) should be chosen to be equal to ($b_{fo}$). The amount of tip flatting ($n$) of the outer front half super-ellipse is chosen to be more than 2 so that the repulsive function can cover more area at the tip of the SPEF in the front of the vehicle. Next, for the inner half super-ellipse which is in the front direction of a vehicle, the length ($a_{fi}$) of the super-ellipse is designed to be

$$a_{fi} = R_U + d_s + d_{min} \tag{2}$$

where $d_{min}$ as in (1), $R_U$ as in Fig. 1, and $d_s$ is the fixed safety distance that is pre-defined to restrict the minimum closest distance between a UAV and obstacles. Note that $a_{fi}$ should be chosen to be less than $a_{fo}$ with enough margin so that the repulsive collision avoidance motion vectors can grow smoothly from zero to its maximum allowed magnitude and also to ensure a technical condition in (4) for not having an infinite collision avoidance motion vector due to the division by zero. This condition is easy to meet and can be satisfied by increasing the distance sensor maximum range or limiting the vehicle speed. For the same reason, the width $b_{fi}$ should be chosen to be less than $b_{fo}$. The length ($a_{bi}$) and width ($b_{bi}$) of the other inner half super-ellipse which is facing to the backward direction a vehicle can be designed in the similar way that we design the outer backward half super-ellipse. The amount of tip flatting ($n$) of the inner front and back half super-ellipse are chosen to be equal to the values of ($n$) of the outer front and back half super-ellipse respectively. Conceptually, the inner two halves of a super-ellipse represent the forbidden region, the shaded region in Fig. 1, in which obstacles should not be in under any circumstances.

Now, let us consider a point that lies in between the inner and outer super-ellipses as shown in Fig. 1. Let $\mathbf{P}_{ro}$ be the distance vector from the center of a UAV to the point and $\mathbf{v}$ be the velocity vector of the UAV. We then define two distance variables $d_i(\mathbf{P}_{ro}, \mathbf{v})$ and $d_o(\mathbf{P}_{ro}, \mathbf{v})$ where $d_i(\mathbf{P}_{ro}, \mathbf{v})$ is the distance from the point to the inner super-ellipse along the direction of $\mathbf{P}_{ro}$ and $d_o(\mathbf{P}_{ro}, \mathbf{v})$ is the distance from the inner super-ellipse to the outer super-ellipse along the direction of $\mathbf{P}_{ro}$. (In the sequel, we use $d_i$ to denote $d_i(\mathbf{P}_{ro}, \mathbf{v})$ and $d_o$ to denote $d_o(\mathbf{P}_{ro}, \mathbf{v})$ for simplicity of notation.) Now, using these two variables, we can represent the relative position of the point with respect to the inner and outer super-ellipses of the SEPF so that the repulsive potential function value can be determined as a function of the ratio $d_i/d_o$. Note that if the point is on the boundary of the outer super-ellipse, then $d_i/d_o = 1$. And if the point is on the boundary of the inner super-ellipse, then $d_i/d_o = 0$.

Let $f : \mathbb{R} \to \mathbb{R}$ be a continuous real-valued function that satisfies two boundary conditions, that are $f(0) = 1$ and $f(1) = 0$. Then we formally define an SEPF ($\mathbf{P}_{rep}$) as:

$$\mathbf{P}_{rep} = \begin{cases} 0, & \text{if } \mathbf{P}_{ro} \text{ outside outer SE} \\ 1, & \text{if } \mathbf{P}_{ro} \text{ inside inner SE} \\ \mu f\left(\frac{d_i(\mathbf{P}_{ro}, \mathbf{v})}{d_o(\mathbf{P}_{ro}, \mathbf{v})}\right), & \text{otherwise} \end{cases} \tag{3}$$

where $\mu$ is a design parameter used to scale the repulsive potential function and SE stands for super-ellipse. In principle, the function $f(\cdot)$ can be any function as long as it is continuous and satisfies both boundary conditions. It could be a linear, quadratic, sine, and cosine function. However, we choose a quadratic function because the magnitude of its gradient, i.e., repulsive collision avoidance motion vector ($\mathbf{V}_{ca}$), evolves linearly form zero at the outer super-ellipse to the required maximum magnitude at the inner super-ellipse. Then, the repulsive potential field becomes

$$\mathbf{P}_{rep} = \begin{cases} 0, & \text{if } \mathbf{P}_{ro} \text{ outside outer SE} \\ 1, & \text{if } \mathbf{P}_{ro} \text{ inside inner SE} \\ \mu\left(\frac{\|\mathbf{P}_{ro}\| - R_i}{R_o - R_i} - 1\right)^2, & \text{otherwise} \end{cases} \tag{4}$$

where $R_o$ and $R_i$ are the distances from the center of a UAV to the outer and inner super-ellipse respectively as shown in Fig. 1. Note that $R_i$ and $R_o$ can be calculated easily using the following super-ellipse equation represented in polar coordinates

$$R = \frac{ab}{\sqrt[n]{|a\cos(\theta)|^n + |b\sin(\theta)|^n}} \tag{5}$$

where $a$, $b$, and $n$ are the length, width, and the amount of tip flattening respectively and $\theta \in [-\pi, \pi]$ is the angle of the vector $\mathbf{P}_{ro}$ with respect to the horizontal axis.

### B. Extension of the SEPF into a 3-Dimensional Space

Since the proposed potential function is designed based on super-ellipses, it is indeed a simple matter to extend the potential function from a 2-dimensional space to a 3-dimensional space. To extend the repulsive SEPF into a 3-dimensional space, we extend $R_U$ in (2) to be the radius of the smallest sphere that encircles the UAV, and $R$ in (5) to be the equation of super-ellipsoid in the spherical coordinates which is given by

$$R = \frac{1}{\sqrt[n]{\left|\frac{\cos(\theta)\sin(\phi)}{a}\right|^n + \left|\frac{\sin(\theta)\sin(\phi)}{b}\right|^n + \left|\frac{\cos(\theta)}{c}\right|^n}} \tag{6}$$

where $a$, $b$, $c$, and $n$ are length, width, height, and the amount of tip flattening respectively and $\theta \in [-\pi, \pi]$, $\phi \in [0, \pi]$ are two angles of a vector represented in spherical coordinate system. The contour slice plot of a 3-dimensional repulsive SEPF is shown in Fig. 2.

## IV. Autonomous Collision Avoidance under Teleoperation

### A. Repulsive Collision Avoidance Vector from an SEPF

The SEPF is designed to provide us with the repulsive collision avoidance motion vector ($\mathbf{V}_{ca}$). The gradient of a

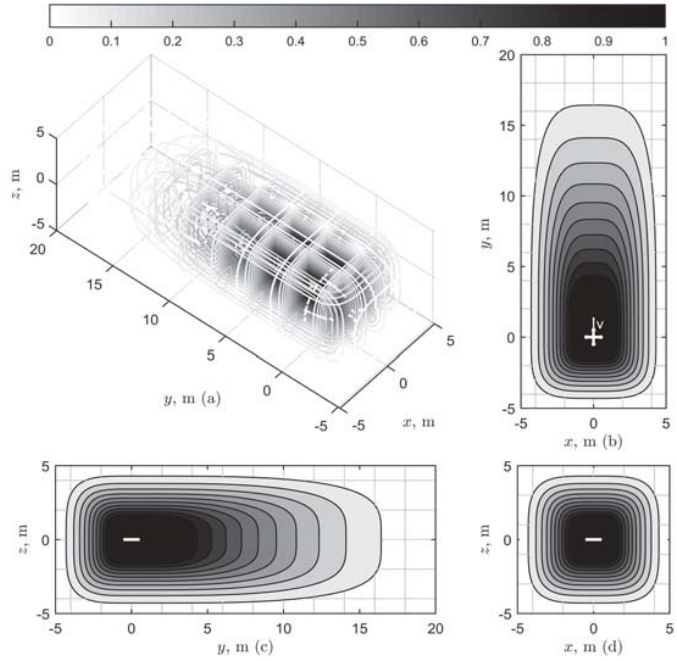


Fig. 2 (a) Contour slice plot of the SEPF with **v**=2 m/s, $a_{fo} = 20$m, $a_{bo} = b_{fo} = b_{bo} = c_{fo} = c_{bo} = 5$m, $b_{fi} = 1.5 + v^2/2a_{max}$, $b_{fi} = c_{fi} = a_{bi} = b_{bi} = c_{bi} = 1.5$, $n = 4$, $\mu = 1$, $a_{max} = 1$. (b) one slice at $z = 0$, (c) one slice at $x = 0$, (c) one slice at $y = 0$

SEPF with respect to the relative position between a vehicle and an obstacle located at ($\mathbf{P}_{ro}$) gives the repulsive collision avoidance motion vector. From the fact that $\nabla_{\mathbf{x}}\|\mathbf{x}\| = \mathbf{x}/\|\mathbf{x}\|$ where $\mathbf{x}$ is a vector, the repulsive collision avoidance motion vector of the SEPF when $\|\mathbf{P}_{ro}\| \in (R_i, R_o)$ is given by

$$\nabla_{\mathbf{P}_{ro}}\Big\{\mu f(\|\mathbf{P}_{ro}\|)\Big\} = \bar{\mu}\Big(\frac{\|\mathbf{P}_{ro}\| - R_i}{R_o - R_i} - 1\Big)\mathbf{n}_{ro} \qquad (7)$$

where the continuous function $f(\cdot)$ is as defined in (4), $\bar{\mu} = 2\mu/(R_o - R_i)$ and $\mathbf{n}_{ro} = \mathbf{P}_{ro}/\|\mathbf{P}_{ro}\|$. Note that the value of $((\|\mathbf{P}_{ro}\| - R_i)/(R_o - R_i) - 1)$ is zero when an obstacle is at the boundary of the outer super-ellipsis and is negative one when an obstacle is on the boundary of inner one. Hence, to make the magnitude of the repulsive vector increases smoothly from zero to a certain positive maximum as an obstacle is getting closer to a vehicle, we need to choose $\mu$ to be a negative, i.e., $\mu < 0$. Furthermore, to ensure the continuity of the repulsive motion vector on the boundary of the inner super-ellipsis, the repulsive collision avoidance motion vector is chosen to be $\bar{\mu}\mathbf{n}_{ro}$. Thus, we finally have the following collision avoidance motion vectors:

$$\mathbf{V}_{ca} = \begin{cases} 0, & \text{if } \mathbf{P}_{ro} \text{ OOSE} \\ \bar{\mu}\mathbf{n}_{ro}, & \text{if } \mathbf{P}_{ro} \text{ IISE} \\ \bar{\mu}\Big(\frac{\|\mathbf{P}_{ro}\| - R_i}{R_o - R_i} - 1\Big)\mathbf{n}_{ro}, & \text{otherwise} \end{cases} \qquad (8)$$

where OOSE and IISE stand for outside outer super-ellipsoid and inside inner supper-ellipsoid simultaneously.

### *B. Repulsive Collision Avoidance Vector from Multiple Points*

The discussion in Section IV-A about the repulsive collision avoidance motion vector ($\mathbf{V}_{ca}$) was for one point on an obstacle. However, a range sensor usually detects a point cloud on the obstacle. There are several ways to combine the multiple repulsive collision avoidance motion vectors. The first simple method is to make the sum of all the repulsive vectors generated from the point cloud. In general, this method results in a large avoidance vector which is undesirable because it restricts the UAV motion. Another method is to calculate the mean of all repulsive vectors generated from the point cloud. This method sometimes leads to a small avoidance vector and a collision may occur because large avoidance vectors are averaged with small avoidance vectors. Finally, we can also make the sum of maximum positive and minimum negative components of repulsive vectors. In this method, the repulsive vectors of a symmetric point cloud around an obstacle will cancel each other. For example, if the UAV is moving perpendicular to the wall, it will stop before hitting the wall because the tangential components to the wall will cancel each other while the normal ones force the vehicle to stop. However, if a UAV is moving towards the wall with an angle, it will deviate its path when approaching to the wall and then move parallel to the wall as shown in Fig. 5. In this paper, we use the last method in the implementation of our simulations presented in Section V.

### *C. Generation of the Reference Velocity Command for a UAV*

In teleoperation, an operator sends control commands to a UAV through a teleoperation device which is an Xbox 360 controller in our case. The control command is considered as a velocity control input ($\mathbf{V}_{in}$) during the simulation in this paper because the control algorithm of the quadrotor UAV requires a velocity control input to work. Now, to generate the control reference input ($\mathbf{V}_{ref}$) to which a UAV should track, the operator control input ($\mathbf{V}_{in}$) and collision avoidance

motion vector ($\mathbf{V}_{ca}$) can be combined together as a simple vector sum, that is

$$\mathbf{V}_{ref} = \mathbf{V}_{in} - \mathbf{V}_{ca} \tag{9}$$

### *D. Directions and Magnitudes of the SEPFs*

In the potential function literature, the direction of a repulsive potential function is in the direction of current vehicle motion. However, in the teleoperation case, this leads to a chattering behavior and the UAV collides with the wall eventually. For example, if a UAV is moving with an angle towards the wall, the vehicle first reach to the closest safety distance $d_s$ to the wall and it continues to move along the wall and hence the SEPF direction is along the wall as well. However, the user control input is still towards the wall and the robot follows it again, but there is not enough time for the repulsive vector to prevent the collision this time, i.e, the wall enters the forbidden region of the SEPF. To address this issue, we assign SEPFs to both the operator's control input direction and current vehicle motion direction as shown in Fig. 3. Now, we have two SEPFs in two different directions and hence the avoidance vectors resulting from them are different as well.

The maximum magnitude of the repulsive vector in the direction of an operator's control input is chosen to be equal to the magnitude of the operator control input, i.e., $\bar{\mu} = \|\mathbf{V}_{in}\|$. The reason for choosing $\bar{\mu}$ to be varying with an operator's control input is to limit the magnitude of the collision avoidance motion vector to the current magnitude of the operator's control input since a large repulsive avoidance vector is not needed when the UAV is commanded to move with a very small velocity. For similar reasons, the maximum magnitude of the avoidance vector in the direction of motion is also chosen to be equal to the magnitude of current vehicle velocity ($\mathbf{v}$), i.e., $\bar{\mu} = \|\mathbf{v}\|$.

## V. Simulation

A human-in-the-loop simulation for the teleoperation of a quadrotor UAV is implemented using the virtual robot experimentation platform (v-rep) in conjunction with Matlab to validate the performance of the proposed autonomous collision avoidance framework using the SEPFs. As shown in Fig. 4, there is a human operator who drives a virtual quadrotor UAV which is implemented inside the v-rep. Also, there is a Matlab program in between the operator and v-rep that is implemented to take input commands from the operator to calculate $\mathbf{V}_{in}$, to receive simulated velocity of the quadrotor UAV as well as sensor data from v-rep to calculate $\mathbf{V}_{ca}$, and finally to perform all necessary calculations to generate a reference velocity $\mathbf{V}_{ref}$ and send it to the v-rep quadrotor UAV model.

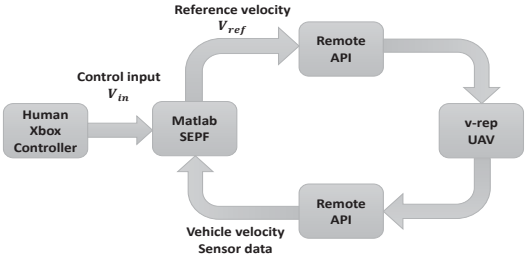


Fig. 4 Simulation diagram showing data transfer between Matlab and v-red and from human operator to Matlab

Fig. 3 shows the case when an operator keeps commanding the quadrotor UAV to move straightforward with its maximum velocity to make the quadrotor UAV collide with the sloped wall in front. As shown in the figure, the quadrotor UAV does not collide with the wall despite of an operator's continuous command in forward direction. Instead, the vehicle continues to follow the operator's command while avoiding collision with the wall. The reason for this behavior is that when the quadrotor UAV comes close to the wall, the velocity vector component in $\mathbf{V}_{in}$ which is perpendicular to the wall is canceled by the vector component in $\mathbf{V}_{ca}$ which is also perpendicular but has opposite direction to avoid collision with the wall. Further, when the quadrotor UAV continues to approach to the left side wall, the blue SEPF constructed along the direction of the vehicle's motion prevents the collision this time, and the vehicle eventually enters the narrow passage without having any collision at all.

In Fig. 5, a quadrotor UAV is driven to approach the right

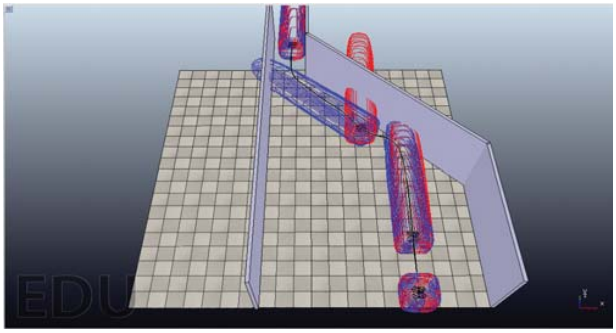

Fig. 3 The quarotor is moving towards a sloped wall: The red SEPF is in the operator command direction while the blue one is in the current motion direction

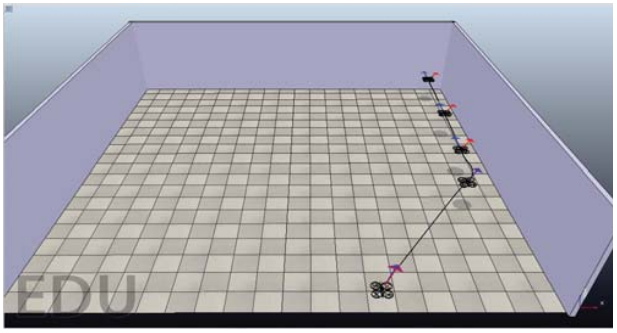

Fig. 5 The quarotor is moving with a skew angle towards the wall: The red arrow is the operator command direction while the blue one is current motion direction

side wall with an angle. As shown in the figure, after the vehicle first reach to the closest safety distance $d_s$ to the wall, it continues to move along the wall without having collision to track the input motion command. When the vehicle reach at the corner, it stops there because the two velocity components $\mathbf{V}_{in}$ and $\mathbf{V}_{ca}$ are now perpendicular to the walls and have same magnitude with opposite directions.

Fig. 6 shows the collision avoidance performance in the $(y-z)$ plane to demonstrate that our algorithm also works in a 3-dimensional space as well.

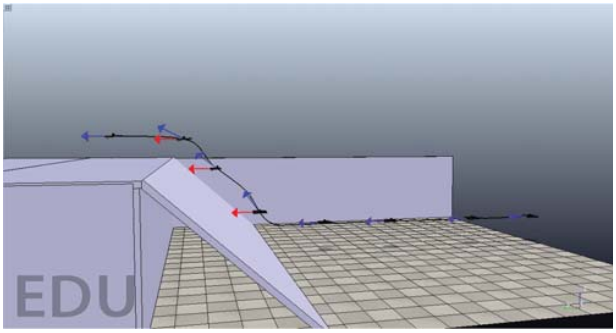


Fig. 6 The quarotor is moving towards a sloped wall: The red arrow is the operator command direction while the blue one is current motion direction

## VI. Conclusion and Future Work

In this paper, a super-ellipsoidal potential function (SEPF) for autonomous collision avoidance of a teleoperated UAV is presented. Simulation results show that a UAV can successfully avoid different kinds obstacles in a 3-dimensional space, while at the same time, follow the operator commands along the obstacle free path. Our method is computationally inexpensive and requires only the relative distance between a UAV and obstacles which can be provided by any range sensor. Implementation of the proposed method on a real quadrotor UAV is currently under progress for experimental validation.

## References

[1] S.R. Barros dos Santos, C.L. Nascimento, S.N. Givigi, "Design of attitude and path tracking controllers for quad-rotor robots using reinforcement learning," in Aerospace Conference, 2012 IEEE , vol., no., pp.1-16, 3-10 March 2012.

[2] R. He, S. Prentice, and N. Roy, Planning in information space for a quadrotor helicopter in a gps-denied environment, in Robotics and Automation, 2008. ICRA 2008. IEEE International Conference on, 2008, pp. 18141820.

[3] L. Garcia-Delgado, A. Dzul, V. Santibanez, M. Llama, "Quad-rotors formation based on potential functions with obstacle avoidance," in Control Theory and Applications, IET , vol.6, no.12, pp.1787-1802, Aug. 16 2012.

[4] B. Hui, S. Shihuang, W. Hongyu, "A VTOL quadrotor platform for multi-UAV path planning," in Electronic and Mechanical Engineering and Information Technology (EMEIT), 2011 International Conference on , vol.6, no., pp.3079-3081, 12-14 Aug. 2011.

[5] C. Masone, A. Franchi, H.H. Bulthoff, P.R. Giordano, "Interactive planning of persistent trajectories for human-assisted navigation of mobile robots," Intelligent Robots and Systems (IROS), 2012 IEEE/RSJ International Conference on , vol., no., pp.2641,2648, 7-12 Oct. 2012.

[6] C. P. G. Niemeyer and G. Hirzinger, Telerobotics, in Springer Handbook of Robotics, B. Siciliano and O. Khatib, Eds. Springer, 2008, pp. 741757.

[7] A. Franchi, C. Secchi, M. Ryll, H.H. Blthoff, and P.R. Giordano, Shared control: Balancing autonomy and human assistance with a group of quadrotor UAVs. IEEE Robotics and Automation Magazine, vol. 19, no. 3, 2012.

[8] T. M. Lam, H. W. Boschloo, M. Mulder, and M. M. V. Paassen, Artificial force field for haptic feedback in UAV teleoperation, IEEE Trans. on Systems, Man, and Cybernetics. Part A: Systems and Humans, vol. 39, no. 6, pp. 13161330, 2009.

[9] N. Diolaiti and C. Melchiorri, Tele-operation of a mobile robot through haptic feedback, in Proc. IEEE Int. Workshop HAVE, Ottawa, ON, Canada, Nov. 1718, 2002, pp. 6772.

[10] P. Stegagno, M. Basile, H.H. Bulthoff, A. Franchi, "A semi-autonomous UAV platform for indoor remote operation with visual and haptic feedback," Robotics and Automation (ICRA), 2014 IEEE International Conference on , vol., no., pp.3862,3869, May 31 2014-June 7 2014.

[11] F. Rehmatullah, J. Kelly, "Vision-Based Collision Avoidance for Personal Aerial Vehicles Using Dynamic Potential Fields," in Computer and Robot Vision (CRV), 2015 12th Conference on , vol., no., pp.297-304, 3-5 June 2015.

[12] M. Nieuwenhuisen, D. Droeschel, J. Schneider, D. Holz, T. Labe, and S. Behnke, Multimodal obstacle detection and collision avoidance for micro aerial vehicles, in Mobile Robots (ECMR), 2013 European Conference on. IEEE, 2013, pp. 712.

[13] C. Masone, P. Robuffo Giordano, H. H. Blthoff, and A. Franchi, Semi-autonomous trajectory generation for mobile robots with integral haptic shared control, in 2014 IEEE Int. Conf. on Robotics and Automation, Hong Kong, China, May. 2014.

[14] S. Stramigioli, R. Mahony, and P. Corke, A novel approach to haptic tele-operation of aerial robot vehicles, in 2010 IEEE Int. Conf. on Robotics and Automation, Anchorage, AK, May 2010, pp. 53025308.

[15] A. Y. Mersha, S. Stramigioli, and R. Carloni, Switching-based mapping and control for haptic teleoperation of aerial robots, in 2012 IEEE/RSJ Int. Conf. on Intelligent Robots and Systems, Vilamoura, Portugal, Oct. 2012, pp. 26292634.

[16] H. Rifa, M. D. Hua, T. Hamel, and P. Morin, Haptic-based bilateral teleoperation of underactuated unmanned aerial vehicles, in 18th IFAC World Congress, Milano, Italy, Aug. 2011, pp. 13 78213 788.

[17] S. Omari, M. D. Hua, G. J. J. Ducard, and T. Hamel, Bilateral haptic teleoperation of VTOL UAVs, in 2013 IEEE Int. Conf. on Robotics and Automation, Karlsruhe, Germany, May 2013, pp. 23852391.

[18] D. Lee, A. Franchi, P. Robuffo Giordano, H. I. Son, and H.H. Blthoff, "Semiautonomous Haptic Teleoperation Control Architecture of Multiple Unmanned Aerial Vehicles," in Mechatronics, IEEE/ASME Transactions on , vol.18, no.4, pp.1334-1345, Aug. 2013.

[19] D. Lee, A. Franchi, P. Robuffo Giordano, H. I. Son, and H.H. Blthoff, Haptic teleoperation of multiple unmanned aerial vehicles over the internet, in 2011 IEEE Int. Conf. on Robotics and Automation, Shanghai, China, May 2011, pp. 13411347.

[20] E. J. Rodriguez-Seda, J. J. Troy, C. A. Erignac, P. Murray, D. M. Stipanovic, and M. W. Spong, Bilateral teleoperation of multiple mobile agents: Coordinated motion and collision avoidance, IEEE Trans. Control Syst. Technol., vol. 18, no. 4, pp. 984992, Jul. 2010.

[21] A. M. Brandt and M. B. Colton, Haptic collision avoidance for a remotely operated quadrotor uav in indoor environments, in Systems Man and Cybernetics (SMC), 2010 IEEE International Conference on, 2010, pp. 27242731.

[22] J. Mendes, R. Ventura, "Safe teleoperation of a quadrotor using FastSLAM," Safety, Security, and Rescue Robotics (SSRR), 2012 IEEE International Symposium on , vol., no., pp.1,6, 5-8 Nov. 2012.

[23] J. Israelsen, M. Beall, D. Bareiss, D. Stuart, E. Keeney, J. van den Berg, "Automatic collision avoidance for manually tele-operated unmanned aerial vehicles," in Robotics and Automation (ICRA), 2014 IEEE International Conference on , vol., no., pp.6638-6643, May 31 2014-June 7 2014.

[24] O. Khatib, Real-time obstacle avoidance for manipulators and mobile robots, Int. J. Robot. Res., vol. 5, no. 1, pp. 9098, 1986.

[25] M. Howie, Choset, "Principles of robot motion: theory, algorithms, and implementation," MIT press, 2005.